

Simulating Heterogeneous Deformation in Polycrystalline Metals using Crystal Plasticity Finite Element Method

Yiyi Yang

School of Engineering, Brown University, Providence, RI 02912, USA

This article provides a general review of fundamentals of crystal plasticity finite element method (CPFEM) and its application in simulating heterogeneous deformation in polycrystalline environment. CPFEM is an important simulation tool for microstructure-based mechanical process prediction, and engineering design involving anisotropic metal material media. Besides a brief discussion of the constitutive laws and kinematics of CPFEM, several of its applications in different deformation processes have also been reviewed, including the uniaxial tension of columnar-grain aluminum, the uni-axial tension of polycrystalline copper, and the four-point bending of polycrystalline titanium, etc. These simulations have all been compared with detailed experimental measurements to validate the accuracy of the applied model.

Key words: CPFEM, computational simulation, plastic deformation, polycrystal

1. Introduction

Heterogeneous deformation in metals, which is commonly viewed as a precursor to damage nucleation, has been crucial topics for decades. Only if the heterogeneous deformation is reliably modeled can locations where cracks form in the first place be properly predicted. Furthermore, from an engineering point of view, knowledge of the micro-crack initiation locations can help to develop processing routes, such as rolling and extrusion, to strengthen metals and alloys by avoiding the development of these locations. The crystal plasticity finite element method (CPFEM) is often used to simulate the plastic deformation processes that occur in three-dimensional microstructures, where the heterogeneous deformation between and within grains co-exists during deformation [1-5].

Heterogeneous deformation usually results from two facts [6-8]. One is that some “soft” grains are much more easily deformed than other grains, which means that one or more deformation systems in the “soft” grains can be more easily activated than those in “hard” grains under certain stress states, leading to large strain differences between soft and hard grains. Secondly, equilibrium across the grain boundary requires an additional stress field along the boundary, resulting from the various

constraints along the grain boundary of a given grain from different neighboring grains during deformation process. Consequently, these influences from neighboring grains can lead to heterogeneous deformation and associated strain gradients within the given grain.

The general framework of CPFEM provides a comprehensive computational tool of continuum mechanics incorporating with the knowledge of physical deformation processes. [9] For example, one of the essential parts in CPFEM framework is that the velocity gradient is described in dyadic form, which reflects the nature of slip and/or twinning shear and consequent shape changes (symmetric part) and lattice rotation (skew-symmetric part). One main advantage of CPFEM is the ability to solve crystal deformation process under complicated boundary conditions, which is crucial for studying heterogeneous deformation within polycrystalline environment and the deformation transfer near interfaces [10, 11]. Also, CPFEM has the flexibility of using different constitutive formulations, according to different materials, to describe plastic flow during deformation in a slip and/or twinning system level [12, 13].

In the first part of this article, the basic constitutive models and kinematics of CPFEM were briefly reviewed. In the second part, several

applications of CPFEM in simulating heterogeneous deformation in polycrystalline materials were introduced. Advantages, challenges and future work on CPFEM were summarized in the last part of the article.

2. Flow kinematic and constitutive models

There are three different coordinate systems in crystal plasticity. Firstly, the shape coordinate system deforms with the total shape change of the specimen during deformation. Secondly, the lattice coordinate system is aligned with the crystallographic directions, and rotates when local lattice rotates, or plastic deformation happens. The difference between shape and lattice distortion is critical to calculate internal stresses [14]. The third coordinate system is the laboratory coordinate system, often used as a reference coordinate system, which is fixed and does not rotate with the body.

The kinematic flow describes the geometrical aspects of the anisotropy of crystals without considering the stresses. The Lagrangian finite strain tensor, \mathbf{E} , is defined by:

$$\mathbf{E} = \frac{1}{2}(\mathbf{F}^T \mathbf{F} - \mathbf{I}) \quad (1)$$

where \mathbf{F} is the deformation gradient, and \mathbf{I} is the second rank identity tensor. The deformation gradient can usually be decomposed into two components, the reversible “elastic” deformation, \mathbf{F}_e , and the irreversible “plastic” deformation, \mathbf{F}_p [15-17]:

$$\mathbf{F} = \mathbf{F}_e \mathbf{F}_p \quad (2)$$

Figure 1 [9] shows an illustration of this decomposition process. When considering a deformation caused by multiple dislocation slip systems, the total deformation gradient can further be decomposed to a series of slip events as:

$$\mathbf{F} = \mathbf{F}_e \left(\mathbf{F}_p^{(n)} \mathbf{F}_p^{(n-1)} \mathbf{F}_p^{(n-2)} \dots \mathbf{F}_p^{(1)} \right) \quad (3)$$

Also, the spatial gradient of the total velocity, \mathbf{L} , which provides the time rate of the change of \mathbf{F} , is

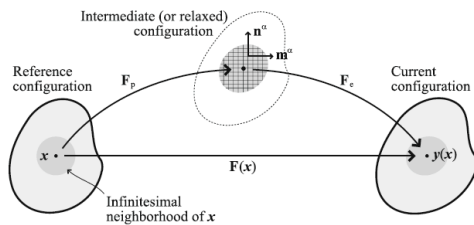


Figure 1. Decomposition of the total deformation gradient [9].

defined as:

$$\mathbf{L} = \dot{\mathbf{F}} \mathbf{F}^{-1} = \dot{\mathbf{F}}_e \mathbf{F}_p^{-1} + \mathbf{F}_e \dot{\mathbf{F}}_p \mathbf{F}_p^{-1} = \mathbf{L}_e + \mathbf{F}_e \mathbf{L}_p \mathbf{F}_e^{-1} \quad (4)$$

In the crystal plasticity, if only considering the dislocation slip as deformation process, the plastic deformation velocity, \mathbf{L}_p , can be defined as the sum of shear rates on all n slip systems:

$$\mathbf{L}_p = \sum_{\alpha=1}^n \dot{\gamma}^\alpha \mathbf{m}^\alpha \otimes \mathbf{n}^\alpha \quad (5)$$

where \mathbf{m}^α and \mathbf{n}^α are the slip direction and the slip plane normal of the slip system α , respectively. $\dot{\gamma}^\alpha$ is the shear rate of the slip system α . This is one of the key equations that combine the crystallographic nature of dislocation slip with conventional finite element method.

The constitutive equations, then, capture the dynamics of slip and/or twinning systems, as carriers of plastic deformation. In other words, the constitutive model defines how the microstructure states within the material will evolve during loading. There are mainly two existing kinds of constitutive models: phenomenological models and physics-based models. In the article, a detailed introduction of phenomenological models is provided, while just a brief review of physics-based models will be given.

2.1 Phenomenological models

Generally, phenomenological constitutive models use the critical resolved shear stress (CRSS) of different deformation system, as state variables. The slip rate of a given deformation system ($\dot{\gamma}^\alpha$) is closely related to the crystallographic nature of the materials, such as CRSS and hardening parameters. When the resolved shear stress of a given system is above its CRSS, the given system will contribute to the total slip rate. On the other hand, if the local stress becomes lower than the CRSS after work hardening, this system will be shut down in the simulation. There are different ways to express the slip rate:

$$\dot{\gamma}^\alpha = \dot{\gamma}_0 \left| \frac{\tau^\alpha}{s^\alpha} \right|^n \text{sgn}(\tau^\alpha) \quad [18-20] \quad (6)$$

or

$$\dot{\gamma}^\alpha = \left| \frac{\tau^\alpha - x^\alpha}{K} - r^\alpha \right|^n \text{sgn}(\tau^\alpha - x^\alpha) \quad [21] \quad (7)$$

where τ^α is the resolved shear stress on the given deformation system. $s^\alpha, x^\alpha, r^\alpha$ are related to CRSS and hardening parameters, the values are time- and/or strain-dependent to reflect the strain

hardening process. The influence of other set of slip system β , on the hardening behavior of slip system α can be described by:

$$\dot{\tau}_c^\alpha = \sum_{\beta=1}^n h_{\alpha\beta} |\dot{\gamma}^\beta| \quad (8)$$

where $h_{\alpha\beta}$ refers to the hardening matrix, which represents the interaction between different slip systems.

These kinds of phenomenological models are currently the most widely used CPFEM models. The disadvantage of these models, however, is the lack of considering lattice defect populations [22,23]. The material state is only described in terms of the CRSS. To overcome this problem, a series of physics-based constitutive models were developed.

2.2 Physics-based models

The physics-based models usually use the dislocation density as the most important state variable during plastic deformation. There are various authors [24-27] having proposed different frameworks to connect the evolution of dislocation density with flow stress during deformation. In this article, only a brief review of these models will be provided.

One good example of these models introduced by Ma et al. [12, 28] uses mobile dislocations, ρ_m^α , gliding along the slip system α to accommodate a part of plastic deformation. These mobile dislocations need to overcome the passing stress introduced by the forest dislocation density, ρ_F^α , as well as the parallel dislocation density, ρ_P^α . The forest dislocations were defined as the dislocations perpendicular to the slip plane of slip system α , while the parallel dislocations as the dislocations parallel to the slip plane. Therefore,

these two dislocation densities can be described using statistically stored dislocation density (ρ_{SSD}^α) in the fcc materials as:

$$\rho_F^\alpha = \sum_{\beta=1}^n \chi^{\alpha\beta} \rho_{SSD}^\beta |\cos(\mathbf{n}^\alpha, \mathbf{t}^\beta)| \quad (9)$$

$$\rho_P^\alpha = \sum_{\beta=1}^n \chi^{\alpha\beta} \rho_{SSD}^\beta |\sin(\mathbf{n}^\alpha, \mathbf{t}^\beta)| \quad (10)$$

where $\chi^{\alpha\beta}$ is the interaction strength between different slip systems. In their model, the effective shear stress can be calculated from the resolved shear stress and the passing stress as:

$$\tau_{eff}^\alpha = |\tau^\alpha| - \tau_{pass}^\alpha = |\tau^\alpha| - c_1 G b \sqrt{\rho_P^\alpha + \rho_m^\alpha} \quad (11)$$

when the resolved shear stress is greater than the passing stress. Otherwise, the effective shear stress will be equal to zero.

There are other physics-based models that also include the geometrically necessary dislocation density, grain size, and grain boundary information directly into the model. These models can effectively simulate the small-scale deformation, such as nano-indentation [29, 30], micropillar compression [31], and micro-beam bending [32].

3. CPFEM applications in simulating heterogeneous deformation

Previous studies [33-36], both experimental and computational, suggested that micro-crack initiate at large strain concentrated locations, where large heterogeneous deformation occurs. However, if the local heterogeneous deformation is large enough to accommodate the local geometry change, or the cohesive energy of a boundary is strong enough [37-40], it will prevent the formation of a micro-crack. Figure 2 provides a schematic description of the relationship between

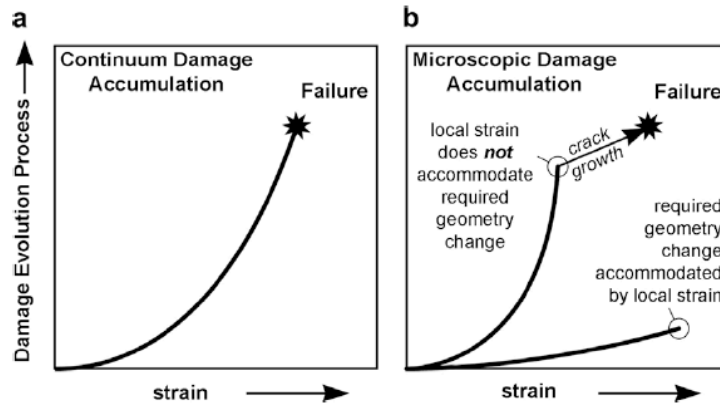


Figure 2. Schematic depiction of relationship between damage and strain in a continuum sense (a), and a comparison of two microstructural scenarios where localized strain causes or prevents damage (b). [41]

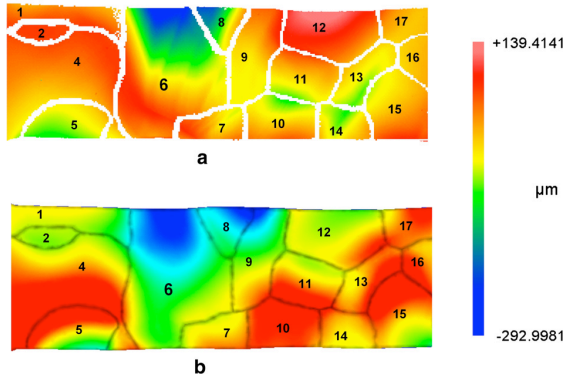


Figure 3. (a) Experimental observation and (b) CPFEM simulated surface roughening profile in an aluminum columnar polycrystal [43].

damage nucleation and strain. In a word, not all large strain sites will be crack initiation sites. Therefore, a detailed study of heterogeneous deformation is essential to understand the crack initiation in polycrystalline metals.

CPFEM is widely used to simulate the plastic deformation processes that occur in three-dimensional microstructures in both cubic metals [42,43] and hexagonal metals [44, 45]. Also, a lot of recent studies have been coupling CPFEM simulation with carefully designed experimental measurements, including surface topography [44], grain rotation [46, 47], local strain mapping [48, 49], etc., to validate the simulation results. Many of these comparisons can be conducted on a one-to-one base. In this section, several selected literature examples of simulating heterogeneous deformation in polycrystalline metals using CPFEM were provided.

3.1 Uniaxial tension of single-layer columnar pure polycrystalline aluminum

Deformation heterogeneities, such as earing and necking, occur during metal forming, which is usually related to the local microstructure and texture of the deformed metals [50, 51]. Zhao et al. [43] performed a study of deformation-induced surface roughening in pure aluminum oligocrystals (a set of coarse grains). In this study, the oligocrystal dog-bone specimen was deformed by uniaxial tension to a final elongation of 15 pct. Grain orientations and grain boundary profile were recorded by electron backscattered diffraction (EBSE) before and after deformation. After deformation, the 3D surface topography of the specimen was measured using a white-light confocal microscope. The explicit phenomenological CPFEM constitutive model first presented by Kuchnicki et al. [52] were used to simulate the

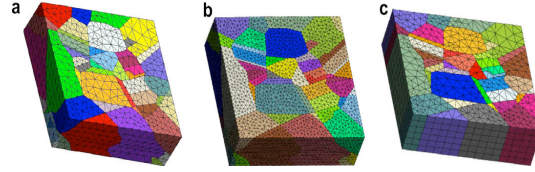


Figure 4. The mesh types used: (a) 3Ds (31,780 nodes), (b) 3Db (130,818 nodes), and (c) quasi-3D (14,076 nodes) [42].

deformation process. Figure 3 shows a very good point-to-point correlation between the measured and simulated surface roughness after deformation. By comparing the experiment measurements and the simulated results, they found that the absence of dislocation barriers provided by grain boundaries is conducive to strain localization. Due to the significant thickness reduction, a severe surface roughening was observed in that region of the sample.

There are some other similar studies on the heterogeneous deformation in coarse grain environment. Similar to the work presented by Zhao et al. [43], these studies [53,54] also indicate strain localization, orientation gradient within a single grain, and heterogeneity depending on grain orientation.

3.2 Uniaxial tension of polycrystalline copper

The studies on single-layer columnar grains summarized in section 3.1 are a prototype to a real 3D simulation. Most of these simulations assume that the grain boundaries are perpendicular to the specimen surface (a quasi-3D mesh), which is usually not valid in real 3D polycrystalline specimens. Recently, some studies have been focused on using CPFEM to simulate deformation processes based on real 3D microstructure of the specimens [55-58]. In a paper published by Musienko et al. [42], a systematic study on the heterogeneous deformation in polycrystalline copper deformed by uniaxial tension were conducted to evaluate the difference between computations using quasi-3D and real 3D meshes. This is one of the only a few papers that directly study the influences of 3D morphology representation in CPFEM. Simulated local deformation behavior using both meshes were also compared with experimental measurements in detail. As shown in Figure 4, three different kinds of meshes were used, a coarse (3Ds) real 3D mesh, a refined (3Db) real 3D mesh, and a quasi-3D mesh. A phenomenological model introduced by Cailletaud [59] was used in the simulation.

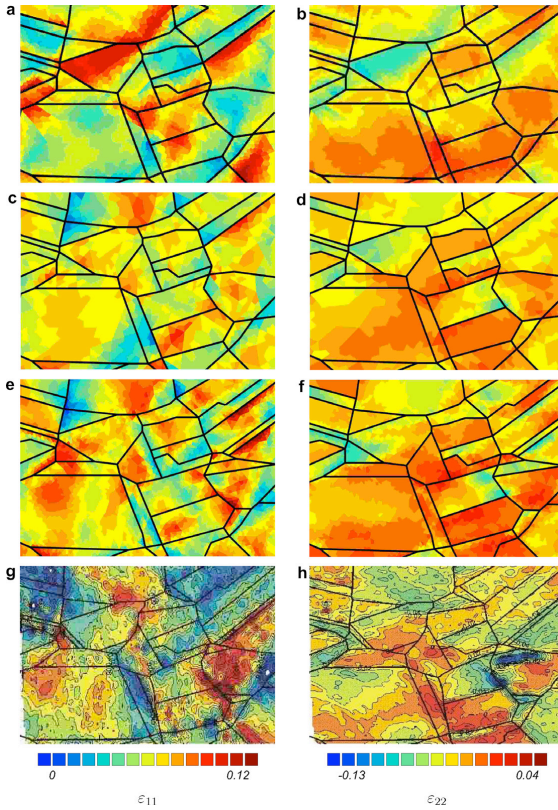


Figure 5. Axial (ϵ_{11}) and transverse (ϵ_{22}) strain fields on the free surface after 5 pct global strain: (a) ϵ_{11} , quasi-3D, (b) ϵ_{22} , quasi-3D, (c) ϵ_{11} , real 3Ds, (d) ϵ_{22} , real 3Ds, (e) ϵ_{11} , real 3Db, (f) ϵ_{22} , real 3Db, (g) ϵ_{11} , experiment, (h) ϵ_{22} , experiment [42].

Experimentally, the strain fields were measured using SEM image correlation. The simulation results shown in Figure 5 clearly indicate that the computational results of the full 3-D mesh are in good agreement with the experimental data. The results for the extended quasi-3D mesh retains some traces of the experimental behavior, but the results are not as good as those obtained with the 3D mesh. The large difference often occurs in smaller grains or at grain boundaries.

This study proved that an accurate representation of the real microstructure is essential to improve the CPFEM simulation results, especially in near grain boundary regions.

3.3 Four-point bending of polycrystalline titanium

Unlike the large amount of work on CPFEM simulations of cubic metals, there are fewer studies on simulating hexagonal metals and comparing these simulated results with experimental measurements. One of the challenges

is that, in hcp metals, there are four different dislocation slip systems and four twinning systems that can be activated during deformation.

In the study reported by Yang et al. [44], the four-point bending process of polycrystalline α -titanium (hcp) were simulated, and validated by a newly developed technique. The specimen were bent to a surface strain at about 1.5 pct. The local shear distribution map for a grain patch (14 grains) was experimentally measured from the step height caused by dislocation and twinning using the technique the author developed combining atomic force microscopy, and electron backscattered diffraction (EBSD). This method allows fine-scale analysis of dislocation activity and derivation of corresponding local shear in the microstructure patch. A phenomenological model proposed by Kuchnicki et al. [52] was applied, and a quasi-3D mesh was used to represent the real grain structure in the study. The twinning activity in this study was treated as a uni-directional dislocation slip. The comparison, as shown in Figure 6, indicated that most of active dislocation slip (especially basal and prismatic slip) and twinning activity were successfully predicted by the model. However, the detailed local shear distribution in hard grains frequently differed from the measurement. Also, the authors found that the existence of a rim outside the real microstructure patch could increase the accuracy of the simulation results in the patch center.

In another paper published by the same group [4], Wang et al. compared the CPFEM results and 3D-XRD measurements of local lattice rotation and activated slip systems during four-point bending of commercial purity titanium. The same of CPFEM framework as that in the last paragraph were used for this study. The results showed the same trend as that found by Yang et al. Dislocation slip activity were partially successful. The crystal rotation, as shown in Figure 7, was poorly captured.

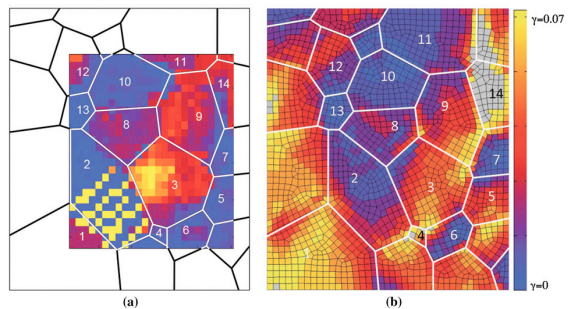


Figure 6. AFM-based (a) experimentally measured and (b) CPFEM simulated sum of all individual local shear distribution maps of the highly characterized microstructure patch.

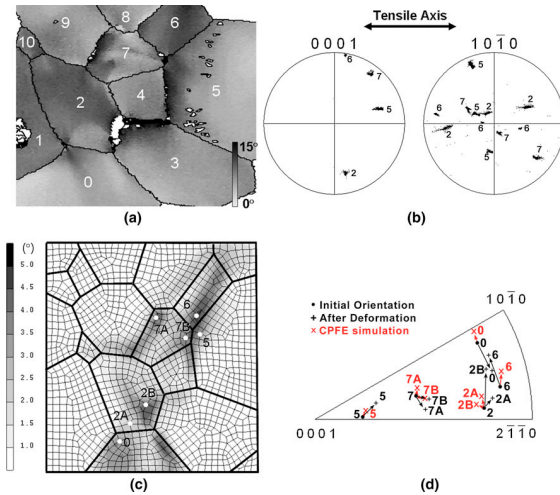


Figure 7. (a) Measured amount of crystal rotation with respect to the initial crystal orientation after 8 pct strain. (b) Pole figures show orientation gradients. (c) Computed amount of crystal rotation after deformation of the microstructure patch. (d) Comparison of crystal rotation directions measured and simulated [4].

These studies indicate that the application of CPFEM in hcp metals still needs further improvement, which may include better representation of 3D microstructure, and better grain boundary and mechanical twinning description in the constitutive models.

4. Challenges and open questions

CPFEM has been proved to be a strong tool that offers a comprehensive approach to simulate various mechanical deformation processes. As shown in the examples in previous sections, there are still critical differences between simulated results and experimental observations. To further increase its accuracy, several main challenges need to be overcome:

- (1) Better representation of microstructure patterning, which includes the formation of dislocation cells, sub-grain structures, martensite, shear bands, etc. A better quantitative description of these structures needs to be developed.
- (2) Better statistical treatments in constitutive models, such as the twinning nucleation and martensite nucleation. Furthermore, as shown in section 3, some metals (fcc or bcc) only show one deformation mechanism, while in other cases, like hcp metals, there is a mixture of dislocation

and twinning activities during deformation. A sub-model describing the interaction of coexisting deformation mechanisms are essential.

- (3) Better simulation of multi-phase alloys. To date, a lot of CPFEM studies were focused on pure metals, and showed relatively good agreement of experimental measurements. The pure metals serve as good prototypes from the academic point of view. In real industry, however, multi-phase alloys are much more widely used due to their better mechanical and chemical properties than that of pure metals. The development of formulations to describe coherent and/or incoherent precipitations [60] and phase boundaries is critical to investigate the mechanical responses of these alloys using CPFEM.

5. Summary

CPFEM is a powerful tool to simulate the various heterogeneous deformation processes with a grain-scale accuracy, which has a wide range of applications in materials science and mechanical engineering. The basic kinematic formulation, constitutive models, and some applications of CPFEM were briefly reviewed in this article. CPFEM allows users to map heterogeneous deformation with detailed knowledge of deformation mechanism, such as dislocation slip, mechanical twinning, martensite formation, and grain boundary sliding, etc. CPFEM is a suitable tool to analyze different mechanical tests because of its strength in predicting the influence of boundary conditions on microstructure evolution. There are, however, still some major challenges to further increase the accuracy of CPFEM prediction.

Acknowledgement

The author is grateful for the financial support from National Science Foundation (NSF), and Army Research Office (ARO).

Reference

- [1] Ma, A., Roters, F., 2004, A constitutive model for fcc single crystals based on dislocation densities and its application to uniaxial compression of aluminum single crystals, *Acta Mater.*, 52(12), 3603-3612.
- [2] Bhattacharyya, A., El-Danaf, E., Kalidindi, S.R., Doherty, R.D., 2001, Evolution of

- grain-scale microstructure during large strain simple compression of polycrystalline aluminum with quasi-columnar grains: OIM measurements and numerical simulations, *Int. J. Plast.*, 17, 861-883.
- [3] Hao, S., Liu, W.K., Moran, B., Vernerey, F., Olson, G.B., 2004, Multi-scale constitutive model and computational framework for the design of ultra-high strength, high toughness steels, *Comput. Methods. Appl. Mech. Eng.*, 193, 1865-1908.
- [4] Wang, L., Barabash, R.I., Yang, Y., Bieler, T.R., Crimp, M.A., Eisenlohr, P., Liu, W., Ice, G.E., 2011, Experimental characterization and crystal plasticity modeling of heterogeneous deformation in polycrystalline α -Ti, *Metall. Mater. Trans. A*, 42(3), 626-635.
- [5] Clayton, J.D., McDowell, D.L., 2004, Homogenized finite elastoplasticity and damage: theory and computations, *Mech. Mater.*, 36, 825-847.
- [6] Lebensohn, R.A., Tome, C.N., 1993, A self-consistent anisotropic approach for the simulation of plastic deformation and texture development of polycrystals: Application to zirconium alloys, *Acta Metall. Mater.*, 41(9), 2611-2624.
- [7] Yao, Z., Wagoner, R.H., 1993, Active slip in aluminum multicrystals, *Acta Metall. Mater.*, 41(2), 451-468.
- [8] Delaire, F., Raphanel, J.L., Rey, C., 2000, Plastic heterogeneities of a copper multicrystal deformed in uniaxial tension: experimental study and finite element simulations, *Acta Mater.*, 48(5), 1075-1087.
- [9] Roters, F., Eisenlohr, P., Hantcherli, L., Tjahjanto, D.D., Bieler, T.R., Raabe, D., 2010, Overview of constitutive laws, kinematics, homogenization and multiscale methods in crystal plasticity finite-element modeling: theory, experiments, applications, *Acta Mater.*, 58, 1152-1211.
- [10] Sachtleber, M., Zhao, Z., Raabe, D., 2002, Experimental investigation of plastic grain interaction, *Mater. Sci. Eng. A*, 336(1-2), 81-87.
- [11] Raabe, D., Sachtleber, M., Weiland, H., Scheele, G., Zhao, Z., 2003, Grain-scale micromechanics of polycrystal surfaces during plastic straining. *Acta Mater.*, 51, 1539-1560.
- [12] Ma, A., Roters, F., Raabe, D., 2006, On the consideration of interactions between dislocations and grain boundaries in crystal plasticity finite element modeling—theory, experiments, and simulations, *Acta Mater.*, 54, 2181–2194.
- [13] Arsenlis, A., Parks, D.M., 1999, Crystallographic aspects of geometrically necessary and statistically-stored dislocation density, *Acta Mater.*, 47, 1597–1611.
- [14] Bilby, B.A., Gardner, L.R.T., Smith, E., 1958, The relation between dislocation density and stress, *Acta Metall.*, 6, 29-33.
- [15] Kroner, E., 1961, On the plastic deformation of polycrystals, *Acta Metal.*, 9, 155-161.
- [16] Lee, E.H., Liu, E.T., 1967, Finite-strain elastic-plastic theory with application to plane-wave analysis, *J. Appl. Phys.*, 38, 19-27.
- [17] Fleck, N.A., Hutchinson, J.W., 1997, Strain gradient plasticity, *Adv. Appl. Mech.*, 33, 1825-1857.
- [18] Kalidindi, S.R., Bhattacharyya, A., Doherty, R.D., 2004, Detailed analyses of grain-scale plastic deformation in columnar polycrystalline aluminum using orientation image mapping and crystal plasticity models, *Proc. Roy. Soc. Lond. A*, 460 (2047), 1935-1956.
- [19] Rice, J.R., 1971, Inelastic constitutive relations for solids: an internal variable theory and its application to metal plasticity, *J. mech. Phys. Solids*, 19, 433-455.
- [20] Hutchinson, J.W., 1976, Bounds and self-consistent estimates for creep of polycrystalline materials, *Proc. Roy. Soc. Lond. A*, 348, 1001-1127.
- [21] Cailletaud, G.A., 1992, A micromechanical approach to inelastic behaviour of metals, *Int. J. Plasticity*, 8(1), 55-73.
- [22] Kocks, U.F., 1966, A statistical theory of flow stress and work-hardening, *Philos. Mag.*, 13, 541.
- [23] Mecking, H., Kocks, U.F., 1986, Kinetics of flow and strain hardening, *Acta. Metall.*, 29, 1865-1875.
- [24] Arsenlis, A., Parks, D.M., Becker, R., Bulatov, V.V., 2004, On the evolution of crystallographic dislocation density in non-homogeneously deforming crystals, *J. Mech. Phys. Solids.*, 52, 1213-1246.
- [25] Arsenlis, A., Parks, D.M., 2002, Modeling the evolution of crystallographic dislocation density in crystal plasticity, *J. Mech. Phys. Solids*, 50, 1979-2009.
- [26] Cheong, K-S., Busso, E.P., 2004, Discrete dislocation density modeling of single phase FCC polycrystal aggregates, *Acta Mater.*, 52, 665-675.

- [27] Gao, H., Huang, Y., 2003, Geometrically necessary dislocation and size-dependent plasticity, *Scripta Mater.*, 48, 113-118.
- [28] Ma, A., Roters, F., 2004, A constitutive model for fcc single crystals based on dislocation densities and its application to uniaxial compression of aluminium single crystals, *Acta Mater.*, 52, 3603-3612.
- [29] Wang, Y., Raabe, D., Kluber, C., Roters, F., 2004, Orientation dependence of nanoindentation pile-up patterns and of nanoindentation microtextures in copper single crystals, *Acta Mater.*, 52, 2229-2238.
- [30] Zaafarani, N., Raabe, D., Singh, R.N., Roters, F., Zaefferer, S., 2006, Three dimensional investigation of the texture and microstructure below a nanoindent in a Cu single crystal using 3D EBSD and crystal plasticity finite element simulations, *Acta Mater.*, 54, 1707-1994.
- [31] Raabe, D., Ma, D., Roters, F., 2007, Effects of initial orientation, sample geometry and friction on anisotropy and crystallographic orientation changes in single crystal microcompression deformation: a crystal plasticity finite element study, *Acta Mater.*, 55, 4567-4583.
- [32] Weber, F., Schestakow, I., Roters, F., Raabe, D., 2008, Texture evolution during bending of a single crystal copper nanowire studied by EBSD and crystal plasticity finite element simulations, *Adv. Eng. Mater.*, 10, 737-741.
- [33] Dunne, F.P.E., Walker, A., Rugg, D., 2007, A systematic study of hcp crystal orientation and morphology effects in polycrystal deformation and fatigue, *Proc. Roy. Soc. Lond. A.*, 463, 1467-1489.
- [34] Bieler, T.R., Fallahi, A., Ng, B.C., Kumar, D., Crimp, M.A., Simkin, B.A., Zamiri, A., Pourboghrat, F., Mason, D.E., 2005, Fracture initiation/propagation parameters for duplex TiAl grain boundaries based on twinning, slip, crystal orientation, and boundary misorientation, *Intermetallics*, 13 (9), 979-984.
- [35] Bieler, T.R., Goetz, R.L., Semiatin, S.L., 2005, Anisotropic plasticity and cavity growth during upset forging of Ti-6Al-4V, *Mater. Sci. Engng. A*, 405, 201-213.
- [36] Querin, J.A., Schneider, J.A., Horstemeyer, M.F., 2007, Analysis of micro void formation at grain boundary triple points in monotonically strained AA6022-T43 sheet metal, *Mater. Sci. Engng. A*, 463, 101-106.
- [37] Palumbo, G., King, P.J., Aust, K.T., Erb, U., Litchenberger, P.C., 1991, Grain-boundary design and control for intergranular stress corrosion resistance, *Scripta Metall. Mater.*, 25, 1775.
- [38] Lejcek, P., Hofmann, S., Paidar, V., 2003, Solute segregation and classification of [100] tilt grain boundaries in alpha-iron: consequences for grain boundary engineering, *Acta Mater.*, 51, 3951-3963.
- [39] McGarrity, E.S., Duxbury, P.M., Holm, E.A., 2005, Statistical physics of grain-boundary engineering, *Phy. Review E*, 71(2), Art. No. 026102, Part 2.
- [40] Randle, V., 2004, Twinning-related grain boundary engineering, *Acta Mater.*, 52, 4067-4081.
- [41] Bieler, T.R., Eisenlohr, P., Roters, F., Kumar, D., Mason, D.E., Crimp, M.A., Raabe, D., 2009, The role of heterogeneous deformation on damage nucleation at grain boundaries in single phase metals, *Int. J. Plasticity*, 25, 1655-1683.
- [42] Musienko, A., Tatschl, A., Schmidegg, K., Kolednik, O., Pippan, R., Cailletaud, G., 2007, Three-dimensional finite element simulation of a polycrystalline copper specimen, *Acta Mater.*, 55, 4121-4136.
- [43] Zhao, Z., Ramesh, M., Raabe, D., Cuitino, A., Radovitzky, R., 2008, Investigation of three-dimensional aspects of grain-scale plastic surface deformation of an aluminum oligocrystal, *Int. J. Plast.*, 24, 2278-2297.
- [44] Yang, Y., Wang, L., Bieler, T.R., Eisenlohr, P., Crimp, M.A., 2011, Quantitative atomic force microscopy characterization and crystal plasticity finite element modeling of heterogeneous deformation in commercial purity titanium, *Metal. Mater. Trans. A*, 42, 636-644.
- [45] Yang, Y., Wang, L., Zambaldi, C., Eisenlohr, P., Barabash, R., Liu, W., Stoudt, M.R., Crimp, M.A., Bieler, T.R., 2011, Characterization and modeling of heterogeneous deformation in commercial purity titanium, *JOM*, 63, 66-73.
- [46] Konrad, J., Zaefferer, S., Raabe, D., 2006, Investigation of orientation gradients around a hard Laves particle in a warm rolled Fe3Al based alloy by a 3D EBSD-FIB technique, *Acta Mater.*, 54, 1369-1380.
- [47] Bate, P.S., Humphreys, F.J., Ridley, N., Zhang, B., 2005, Microstructure and texture evolution in the tension of superplastic Al-6Cu-0.4Zr, *Acta Mater.*, 53, 3059-3069.
- [48] Rehrl, C., Kleber, S., Antretter, T., Pippan, R., 2011, A methodology to study crystal plasticity inside a compression test sample

- based on image correlation and EBSD, *Mater. Char.*, 62, 793-800.
- [49] Delaire, F., Raphanel, J.L., Rey, C., 2000, Plastic heterogeneities of a copper multicrystal deformed in uniaxial tension: experimental study and finite element simulations, *Acta Mater.*, 48(5), 1075-1087.
- [50] Becker, R., 1998, Effects of strain localization on surface roughening during sheet forming, *Acta Mater.*, 46, 1385-1401.
- [51] Zhang, N., Tong, W., 2004, An experimental study on grain deformation and interactions in an Al-0.5%Mg multicrystal, *Int. J. Plasticity*, 20, 523-542.
- [52] Kuchnicki, S.N., Cuitino, A.M., Radovitzky, R.A., 2006, Efficient and robust constitutive integrators for single-crystal plasticity modeling, *Int. J. Plasticity*, 22, 1988-2011.
- [53] Sachtleber, M., Zhao, Z., Raabe, D., 2002, Experimental investigation of plastic grain interaction, *Mater. Sci. Eng. A*, 336, 81-87.
- [54] Beaudoin, A.J., Mecking, H., Kocks, U.F., 1996, Development of localized orientation gradients in fcc polycrystals, *Philos. Mag. A*, 73, 1503-1517.
- [55] Ludwig, W., King, A., Reischig, P., Herbig, M., Lauridsen, E.M., Schmidt, S., Proudhon, H., Forest, S., Cloetens, P., Rolland du Roscoat, S., Buffiere, J.Y., Marrow, T.J., Poulsen, H.F., 2009, New opportunities for 3D materials science of polycrystalline materials at the micrometer lengthscale by combined use of X-ray diffraction and X-ray imaging, *Mater. Sci. Engng. A*, 524, 69-76.
- [56] Rossiter, J., Brahme, A., Inal, K., Mishra, R., 2013, Numerical analyses of surface roughness during bending of FCC single crystals and polycrystals, *Int. J. Plasticity*, 46, 82-93.
- [57] Barbe, F., Decker, L., Jeulin, D., Cailletaud, G., 2001, Intergranular and intragranular behavior of polycrystalline aggregates. Part 1: FE model, *Int. J. Plasticity*, 17, 513-536.
- [58] Barbe, F., Decker, L., Jeulin, D., Cailletaud, G., 2001, Intergranular and intragranular behavior of polycrystalline aggregates. Part 2: Results, *Int. J. Plasticity*, 17, 537-563.
- [59] Cailletaud, G., 1992, A micromechanical approach to inelastic behaviour of metals. *Int. J. Plasticity*, 8, 55-73.
- [60] Zambaldi, C., Roters, F., Raabe, D., Glatzel, U., 2007, Modeling and experiments on the indentation deformation and recrystallization of a single-crystal nickel-base superalloy, *Mater. Sci. Eng. A*, 454-455.